Marine and Petroleum Geology 133 (2021) 105292

Contents lists available at ScienceDirect

Marine and Petroleum Geology

journal homepage: www.elsevier.com/locate/marpetgeo

# Interpretation of aeromagnetic data to detect the deep-seated basement faults in fold thrust belts: NW part of the petroliferous Fars province, Zagros belt, Iran

Raana Razavi Pash [a], Zeinab Davoodi [b], Soumyajit Mukherjee [c,*], Leila Hashemi Dehsarvi [a], Tahereh Ghasemi-Rozveh [d]

[a] Department of Earth Sciences, College of Sciences, Shiraz University, Shiraz, Iran
[b] Department of Geology, Faculty of Science, Imam Khomeini International University, Qazvin, Iran
[c] Department of Earth Sciences, Indian Institute of Technology Bombay, Powai, Mumbai, 400 076, Maharashtra, India
[d] Department of Earth Sciences, College of Sciences, Birjand University, Birjand, Iran

ARTICLE INFO

*Keywords:*
Aeromagnetic data
Tilt filtering
Deep-seated basement fault
Zagros belt
Fars province

ABSTRACT

Detection and delineation of basement faults are fundamental exercises in petroleum geology. This is because such structures can guide later deformation and the associated structures within the younger overlying sediments. This work presents aeromagnetic data interpretation and a comparison with the Digital Elevation Model (DEM) to detect basement structures covering the NW part of the petroliferous Fars province, Zagros belt. Anticlinal axes deflect in the NW-part of the province. The reason for this deflection is debated. We identified basement faults from the airborne geomagnetic data. Tilt filtering was applied on the magnetic data to enhance such faults. Two NE-trending cross-sections perpendicular to the anticlinal axes were prepared to show the effect of the basement faults in the sequence stratigraphy. The results of this research indicate a major NW and another NE trending deep-seated fault. Most of the extracted magnetic lineaments correspond to these faults. These faults were confirmed by the high displacement of the layers and changes of the thickness in the sequence stratigraphy. The result of this research suggests that the deep-seated basement faults are the main controlling factor of structural style in the NW part of Fars province in terms of a thick-skinned tectonics.

## 1. Introduction

Two contrasting views have been available for interpretation of the main controlling factors of the structural styles in the Zagros Fold Thrust Belt, especially in the Fars province. One states that the Hormuz salt (basal decollement) as the salt diapir has an important role in the structural style (due to the deflection of the fold axes on the surface) especially in the Fars province (e.g., Letouzey and Sherkati, 2004). Analogue models of Bahroudi et al. (2003) and Jahani et al. (2009) show that the surficial faults or deflection along the folds could be due to salt diapirsim the sedimentary cover without any relationship with the basement faults. The other view is that the basement might also be deformed (e.g., Lacombe and Mouthereau, 2002; Mouthereau et al., 2007; Lacombe and Bellahsen, 2016; Koyi et al., 2016) and that the basement faulting is the main controlling factor for the deformation for the overlying materials (Misra et al., 2014; Misra and Mukherjee, 2015). These two possibilities, the thin-skinned and the thick-skinned tectonics, are likely to compete in the Zagros belt (Fig. 1). Seismotectonic studies have provided more reliable evidence for the thick-skinned deformation and the role of the basement faulting as the main controlling factor in the changes of surficial features (Jackson, 1980; Ni and Barazangi, 1986; Berberian, 1995).

Analogue models show that the superficial features or deflection along the folds could also be related to the presence of the deep-seated basement faults in the Fars province (Koyi et al., 2016). These models indicate that the deflection of the fold axis from NW-SE trending in the western part of the Fars province to the E-W trend in the eastern part are related to the rotation of the deep-seated basement faults. In other words, basement faults have been considered to be the main controlling factor of the structural style in the region.

The Fars region has been a critical location where several concepts of Zagros orogeny have come up (Sarkarinejad et al., 2018a, 2018b). Based

* Corresponding author.
*E-mail addresses:* soumyajitm@gmail.com, smukherjee@iitb.ac.in (S. Mukherjee).

https://doi.org/10.1016/j.marpetgeo.2021.105292
Received 18 May 2021; Received in revised form 10 August 2021; Accepted 10 August 2021
Available online 13 August 2021
0264-8172/

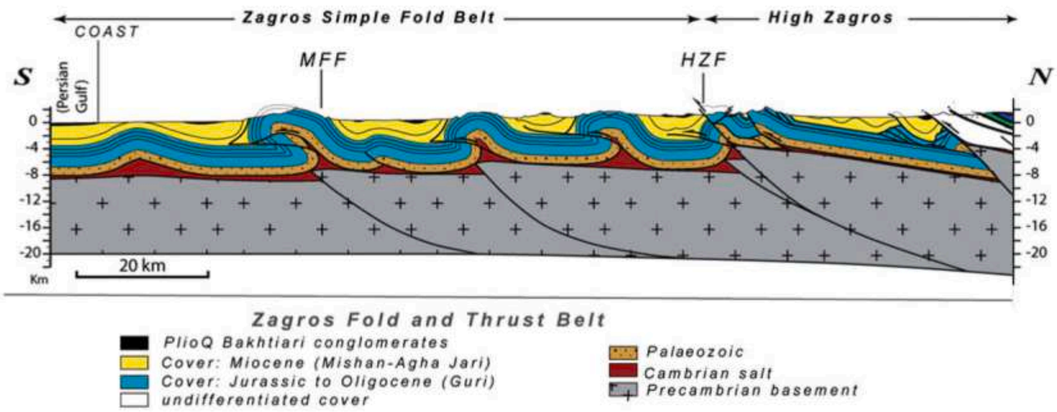


**Fig. 1.** Schematic thick-skinned and thin-skinned tectonics in the central Zagros (Agard et al., 2011). In some parts of this section, the basement is not involved with the deformation, but in some other parts, it is, especially towards the high Zagros where the thickness of basal decollement decreased. MFF: Mountain Front Fault and HZF: High Zagros Fault.

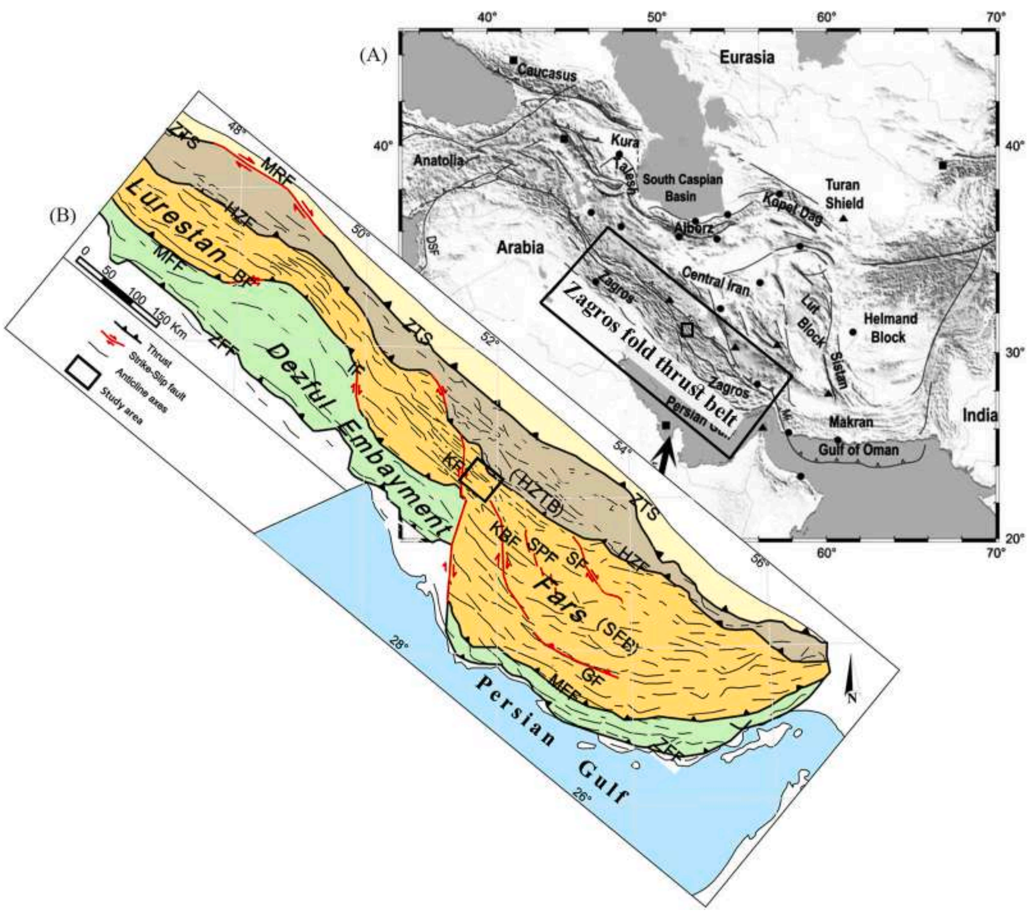


**Fig. 2.** Structural map and subdivision of the Zagros belt and location of the study area, Compiled from HuberH (1977), Berberian (1995) and Sepehr and Cosgrove (2005). ZTS: Zagros Thrust System, MRF: Main Recent Fault, HZF: High Zagros Fault, MFF: Mountain Front Fault, ZFF: Zagros Foredeep Fault, BF: Bala Rud Fault, IF: Izeh Fault, KF: Kazerun Fault, KBF: Kar-e-Bass Fault, SPF: Sabz-Pushan Fault, SF: Sarvestan Fault, GF: Ghir Fault.

on stratigraphic data, during Zagros orogeny in the Early Miocene, inversion of the pre-existing structural elements with N–S and NW-SE trending is the first stage of the deformation in the Fars region (Mouthereau et al., 2007). The relationship between the surficial deformation of the anticlines and the basement faults in the study area so far remained doubtful. This is because such faults have not been documented in the NW part of the Fars province.

In this article, the basement faults are detected using filtering of magnetic data in the southern part of Iran, at the NW part of the Fars province. Also, the effect of these faults is investigated at the surface and through stratigraphy. The deflection and offset of anticlines at the surface are investigated in relation to the detected basement faults.

## 2. Study area

The study area is located within longitudes 51° 32′ to 53° 59′ E and

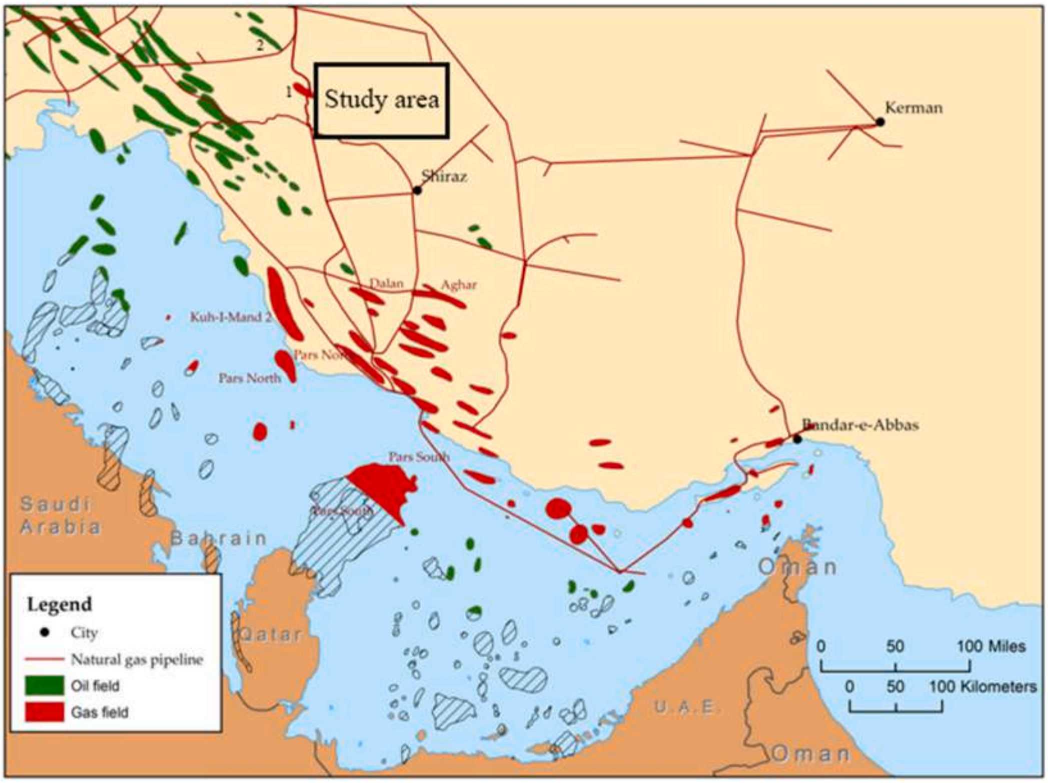


**Fig. 3.** The distribution of gas and oil fields in the Fars province. Oil and gas fields close to the study area are marked with a number (1: Mokhtar gas field and 2: Shurom oil field).

**Table 1**
A list of references related to the methods of interpreting magnetic data.

| Reference | Studied terrain | Findings |
|---|---|---|
| Lyatsky et al. (2004) | The Alberta Basin, Canada | Detection of subtle basement faults with gravity and magnetic data |
| Salem et al. (2008) | Method | Tilt filtering of Magnetic data method is powerful method for detection of the basement fault |
| Crawford et al. (2010) | The Wernecke Inlier, Yukon Territory, Canada | Structural connectivity between basement faults and mapped normal faults lead to detect fluid pathways during ca. 1590 Ma hydrothermal activity |
| Ndougsa-Mbarga at al. (2012) | Eburnean orogeny, SE Cameroon | Deep tectonic features in basement using aeromagnetic data |
| Arisoy and Dikmen (2013) | Method | Total horizontal derivative of the tilt angle is valuable method for edge detection of magnetic sources |
| Shah and Crain (2018) | The crystalline basement in north-central Oklahoma | Significant structural differences between the crystalline basement and sedimentary cover, numerous seismogenic faults, and highlighting previously unmapped basement faults or contacts |
| Ibraheem et al. (2019) | Sohag Area, Egypt | The result helps making decision in choosing the location of the boreholes for gas and oil exploration. |
| Ariyo et al. (2020) | Precambrian gneisses of Ago-Iwoye, southwestern Nigeria | A prospective hydro-geological center, fault zones according to Liberian orogenic compression and as an undesirable spot for high-rise building |

latitudes 29° 29′ to 31° 29′ N, in the Zagros Mountains, NW part of Fars province, Iran (Fig. 2). There are several gas fields in the Fars province that explore hydrocarbons from the Dehram Group (Kangan and Dalan equivalent to Khouf Formations as reservoir layers) from ~2600 to 5311 m depth (Rouhani and Zakeri, 2012) (Fig. 3). The deflection of the anticlinal axes is visible at the surface in the NW part of the province. However, the reason for the swing is not well understood. No salt diapirs have so far been mapped (Mouthereau et al., 2007; JahaniS, 2009) between the NW-trending High Zagros Fault and the N-trending Kazerun Fault. The thickness of the Hormuz salt is very low in the northern Fars province and is devoid of diapirs (Sherkati et al., 2006).

## 3. Geophysical background

Aeromagnetic data has classically been used for economic surveys (Blakely, 1995) and recently in the structural mapping (Saibi et al., 2016). The initial problems of structural mapping of a magnetic crystalline basement overlain by the non-magnetic sedimentary rocks have long been solved by the different methods of magnetic interpretation (review in Table 1).

Geophysicists define the basement based on the reflectivity pattern or physical properties (e.g., seismic wave velocities, magnetic or gravimetric signature) and compare them with those of the overlying sedimentary rocks (Lacombe and Bellahsen, 2016). Numerous geophysical studies have been performed worldwide to extract the basement faults using magnetic data (review in Table 2). The depth to the top of fresh igneous rocks is often named the magnetic basement. Sedimentary rocks are considered non-magnetic. In other words, the igneous basement is considerably more magnetized than the overlying sediments (Teknik and Ghods, 2017). No magnetic layers occur within the sedimentary package in the study area (in the NW part of Fars province). Lack of intrastriatal magnetic material is also the case with theZagros belt. The magnetic map can be the base map for the extraction of the basement faults in Zagros (Bahroudi and Talbot, 2003).

**Table 2**
List of references related to the detection of basement faulting using magnetic methods.

| Reference | Studied terrain | Findings |
|---|---|---|
| Cordell and Grauch (1985) | San Juan basin, New, Mexico | The detection of magnetization boundaries using linear filter based on the gradient of pseudogravity |
| Jacobi (2002) | the Appalachian Basin of, New York State | Not only are there more faults than previously suspected in NYS, but also, many of these faults are seismically active. |
| Lyatsky et al. (2004) | The Alberta Basin, Canada | Detection of subtle basement faults with gravity and magnetic data |
| Crawford et al. (2010) | The Wernecke Inlier, Yukon Territory, Canada | structural connectivity between basement faults and mapped normal faults lead to detect fluid pathways during ca. 1590 Ma hydrothermal activity |
| Wang et al. (2015) | The Ordos hydrocarbon basin, North China Craton (NCC) | The result from integrated aeromagnetic and geological data indicate the Ordos block is not an entirety of Archean. |
| Lin et al. (2015) | The Tarim Basin, China | Basement faults are syn-depositional with continuous long-term activity during the basin's evolution |
| Ali et al. (2017) | The UAE basin, United Arab Emirate | Hydrocarbon distribution in the UAE basin appears to be controlled by the location of the basement ridges |
| Lenhart et al. (2019) | The Måløy Slope, offshore west Norway | Structural architecture and composition of the crystalline basement as the indicator for location of the suture zone between Baltica and Laurentia |
| Geng et al. (2020) | Offshore Abu Dhabi, United Arab Emirates | The giant oilfields and smaller oilfields in offshore Abu Dhabi, occur exactly above crests of salt pillows and at the margin of the northern basement high respectively. The basement morphology and mobilization of the Hormuz salts due to reactivation of the basements fault. |
| Ikioda et al. (2021) | Anambra Basin, Nigeria | Determine the structural pattern and sedimentary thickness of the basin |

## 4. Geology and tectonics

Iran is located within the active convergence zone between the Arabian and the Eurasian plates (Fig. 4A). In this country, the Arabia-Eurasia convergence trends N to NNE. Estimates of its velocity range from 22 mm $yr^{-1}$ (Bayer et al. 2002) to 35 mm $yr^{-1}$ (DeMets et al., 1990). The most reliable convergence vector is provided by the recent GPS studies at the Arabian plate scale and corresponds to a velocity of ~22–25 mm $y^{-1}$ towards N010°E (McClusky et al., 2003; Vernant et al., 2004; Lacombe and Mouthereau et al., 2006; Masson et al., 2007, Fig. 5). The direction is oblique by ~ 20–30° to the principal long-term SW–NE shortening direction across the orogen (Agard et al., 2011). The northward convergence has accommodated a dextral strike-slip on the Main Recent Fault (Talebian and Jackson, 2004; Authemayou et al., 2009), the Kazerun Fault (Authemayou et al. 2006, 2009) and sub-ordinate faults of the Kazerun Fault (Lacombe et al., 2006). Overall, the direction of the convergence vector has controlled the deformation partitioning along the orogen (Fig. 4A). The exposed lithologies in the geologic maps in the study area are the Tertiary and the Quaternary deposits (Fig. 4B).

The Zagros Fold and Thrust Belt (ZFTB) is ~1800 km in length, and is formed in the foreland of the collision zone between the Arabian and the Eurasian plates. The belt is a part of the Alpine-Himalayan orogenic system that evolved during the initiation and the closure stages of the Neotethys Ocean at the Tertiary time (e.g., RicouL, 1971; Lacombe et al., 2011). The ZFTB has three provinces, towards SE these are: Lurestan province, Dezful embayment and the Fars province.

Within the Late Proterozoic to Pleistocene ~ 7–14 km in the thick sedimentary pile of the Zagros belt (Karasozen et al. 2018) and multiple décollement levels complicate the deformation in the sedimentary cover and hides the subsurface faults (Sherkati et al., 2006). The effect of subsurface faults at the surface is manifested as clockwise ~$70^0$ rotation and several km of displacement of fold axes in the Fars province (Koyi et al., 2016). In this province, the main décollement levels are the Dashtak and the Hormuz salt Formations (Sherkati et al., 2006) (Fig. 5). In the study area, the Hormuz salt is the main décollementat the base of the sedimentary cover (Mukherjee et al., 2010).

NW-trending faults and folds are the main structures in the Fars province. Towards the east of this province, structural trend swings to E-W. The Kareh Bas, Sabz-Pushan, Sarvestan, and Ghir Fault Zones are the master blind faults in the Fars province (Berberian, 1995, Fig. 2). The E-trending Ghir Fault is the SW–verging thrust (Sarkarinejad et al., 2018a, 2018b). The other three faults trend N and display a right-lateral mechanism (e.g., HuberH, 1977; Sepehr and Cosgrove, 2005). Whether any basement faults exist in the NW part of Fars province between the Kazerun Fault and the High Zagros Fault has remained indeterminate.

## 5. Methods

### 5.1. General points

Aeromagnetic data, acquired by the Geological Survey of Iran aerially from~ 343 m height, were used to detect the magnetic lineaments. The survey was conducted by the Aeroservice Company (Houston, Texas, USA) under the commission from the Geological Survey of Iran during 1974–1977. The survey was done using a twin-engine airplane by a cesium vapor magnetometer with a sensitivity of 0.02 gammas. The data were collected along the flight lines with an average line spacing of 7.5 km. The average spacing of the control flight lines was 40 km (Saleh, 2006).

Long-wavelength data of the magnetic intensity field were used since these data often correspond to deeper-crustal sources (Ten Brink et al. 2007). Oasis montajGeosoft software (Version 9.5, 2018) designed by the Geosoft Company was used to process the data. First, the aeromagnetic map was prepared using the aeromagnetic data (Fig. 6). This map is the basis for the interpretation of the magnetic lineaments and indicates different magnetic anomalies.

Information about the magnetic lineaments was obtained using filtering. Evidence of faulting along these detected lineaments were investigated using the tilt filtering map, Digital Elevation Model (DEM; prepared using the GIS software, version 10.5) and structural cross-sections (prepared using the 2D Move software, version 2013). Finally, a structural map of the study area was prepared using interpretation results of the filtering. In this map, the extracted basement faults (F1–F6) in this research were drawn.

The DEM is used to indicate the effect of the basement faults at the surface. This approach essentially relies on identifying the deflection of the fold's axes and the offset of the markers (Saibi et al., 2016).

### 5.2. Tilt filtering

Airborne geophysical data must be filtered by the tilt filtering to detect regionally the lineaments and fractures. This filter is an upward filter normalizing the vertical deviation with respect to the horizontal deviation. Since the output in this filter is normalized in the range of 90° to −90°, deep and surficial anomalies are detected uniformly. Deep and surficial structures are observed after that in terms of uniform anomalies (Miller and Singh, 1994). The tilt angle ($\theta$) is defined as:

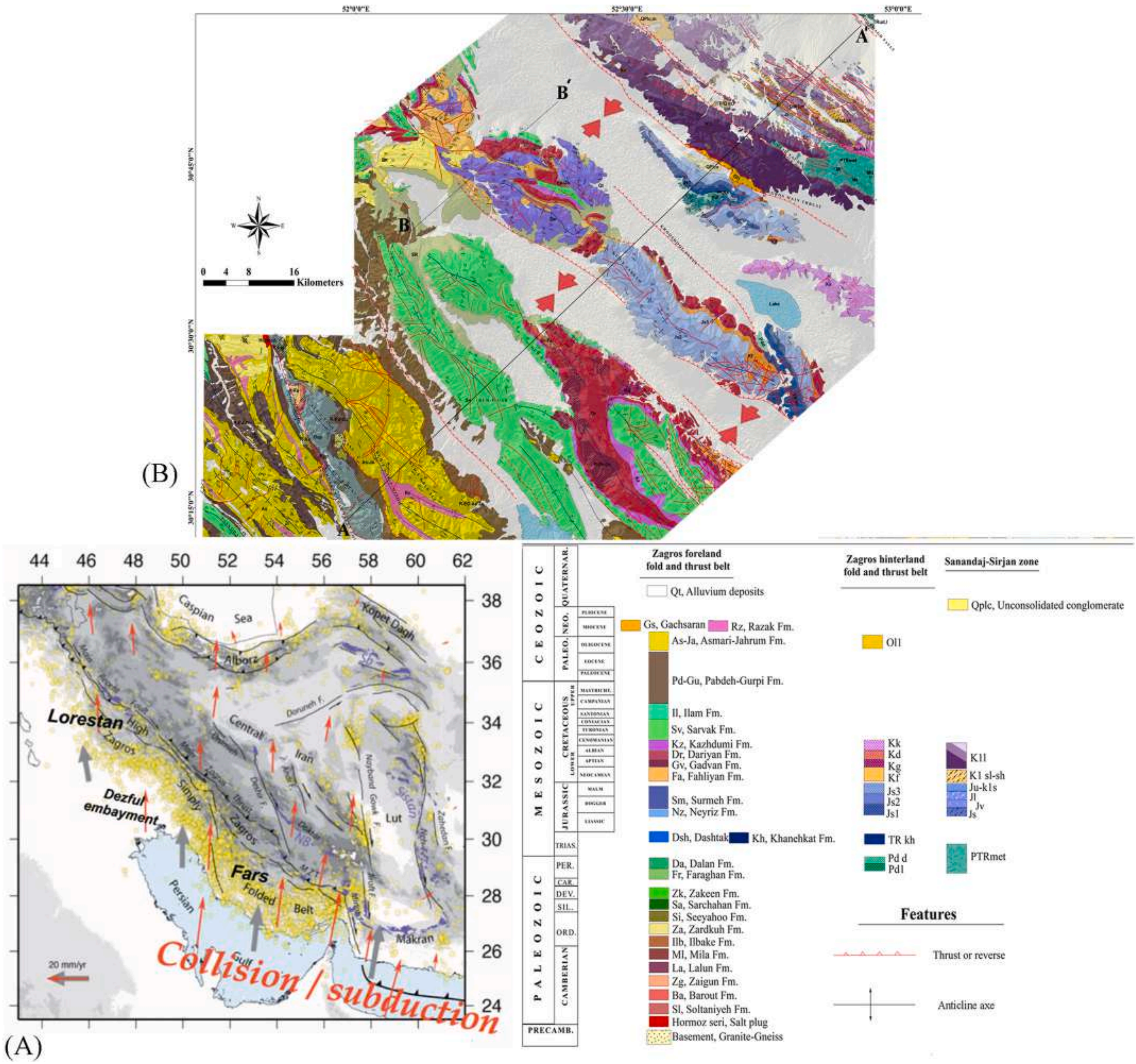


**Fig. 4.** (A) Present-day deformation of Iran, as seen through seismicity (yellow dots) and the location of major active faults (for deformation partitioning) (Agard et al., 2011). GPS vectors are shown in red. The direction of the convergence vector has been controlled by the deformation partitioning across Iran as shown in Fig. 5A.(B) Simplified geologic map of the study area, taken from 1:100000 scaled maps of Geological Survey of Iran and National Iranian Oil Operating Company. Along AA′ and BB′, cross-sections have been presented in Fig. 8. (For interpretation of the references to color in this figure legend, the reader is referred to the Web version of this article.)

$$\theta=\tan^{-1}\left[\frac{\frac{\partial z}{\partial M}}{\partial h}\right] \tag{1}$$

$$\frac{\partial M}{\partial h}=\sqrt{\left(\frac{\partial M}{\partial x}+\frac{\partial M}{\partial y}\right)^{2}} \tag{2}$$

Here M is the total magnetic field, ∂M/∂Z is the vertical deviation field and ∂M/∂Y and ∂M/∂X are the horizontal deviations along X and Y-axes, respectively (Verduzco et al., 2004).

Tilt is zero at the boundary on the positive anomalies and it is negative outside the anomalies range. Thus, the zero value marks the anomaly's boundary

$$\theta=\tan^{-1}\left[\frac{h}{Z_c}\right] \tag{3}$$

In Equation (3), h and $z_c$ are the horizontal location and depth of the magnetic field, respectively. This equation indicates that $\theta = 0^{\circ}$ (*for* $h = 0$) above the edges of the contact and equals $\pm 45^{\circ}$ for $h = \pm z_c$. The contours of the magnetic tilt angle can identify both the location ($\theta = 0^{\circ}$) and depth (half the physical distance between $\pm 45^{\circ}$ contours) of the contact-like structures (Salem et al., 2007, 2008).

Tilt filtering was performed on the Reduction To Pole (RTP). Also, the upward filter was performed on the RTP to remove the surficial noise for better investigation of the deep magnetic bodies. RTP transformation was applied to the magnetic data to minimize the polarity effects

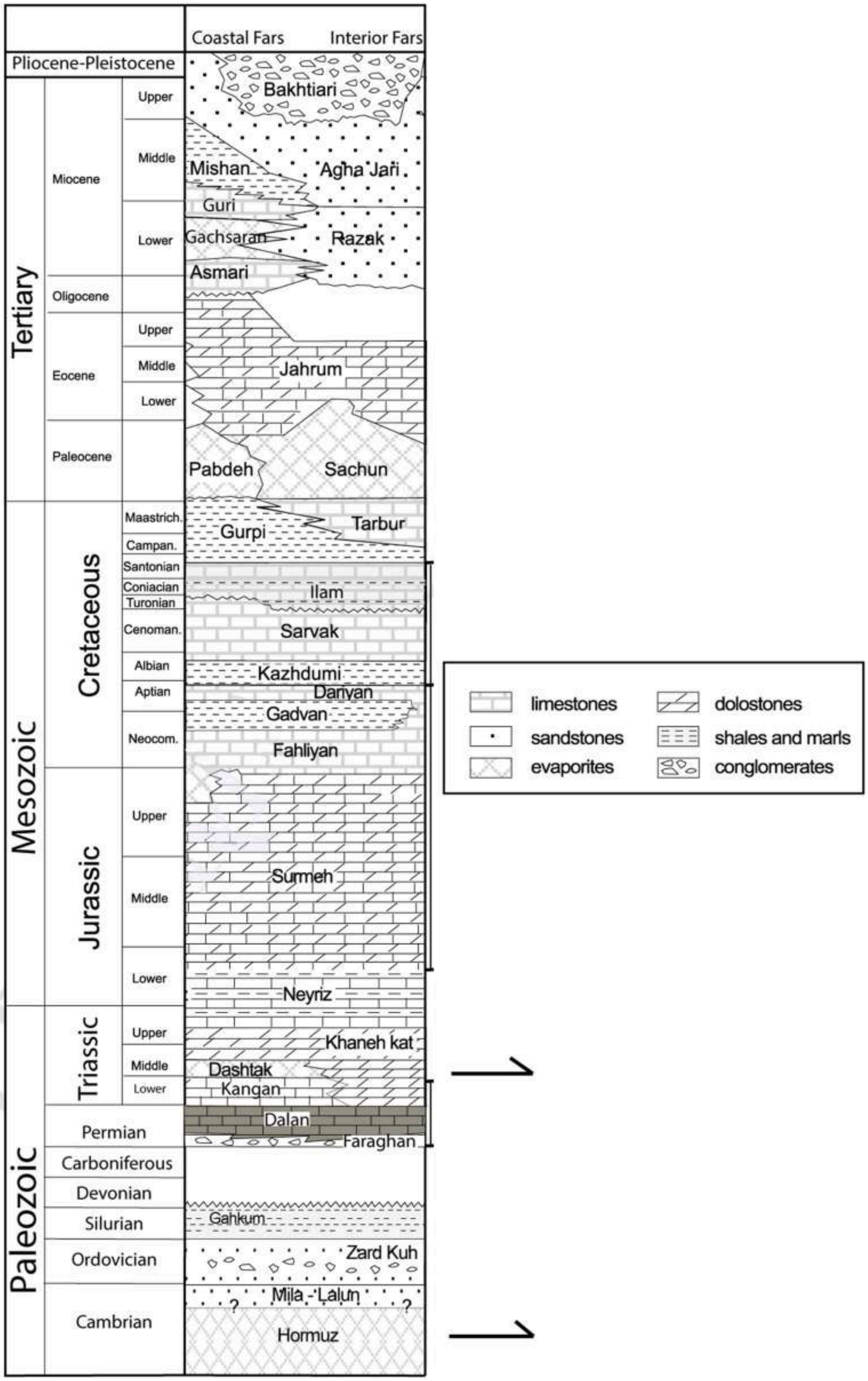


**Fig. 5.** Stratigraphic column of the Fars province. Possible décollement levels within the sedimentary succession are shown with thick black arrows. The Hormuz salt is main basal décollement level in the Fars province (Sherkati et al., 2006; Lacombe and Mouthereau 2006; Agardetal. 2011; Najafi et al., 2014).

(Blakely, 1995). These effects are manifested as a shift of the main anomaly from the center of the magnetic source and result from the vector nature of the measured magnetic field. These filters are considered the most useful for defining the edges of bodies and amplifying the fault trends. The tilt filtering was performed on the magnetic data after processing the data. Two TDR (tilt derivative) and HD– TDR (horizontal tilt derivative) maps are the outputs of the tilt filtering (Fig. 7). The body's boundaries are easily defined in the TDR map and, the lineaments are simply defined in the HD - TDR map.

The presence of a magnetic lineament does not always confirm a fault. Mostly, the basement lithology, granite-gneiss rocks in the present case, has more effect on the magnetic relief observed above the

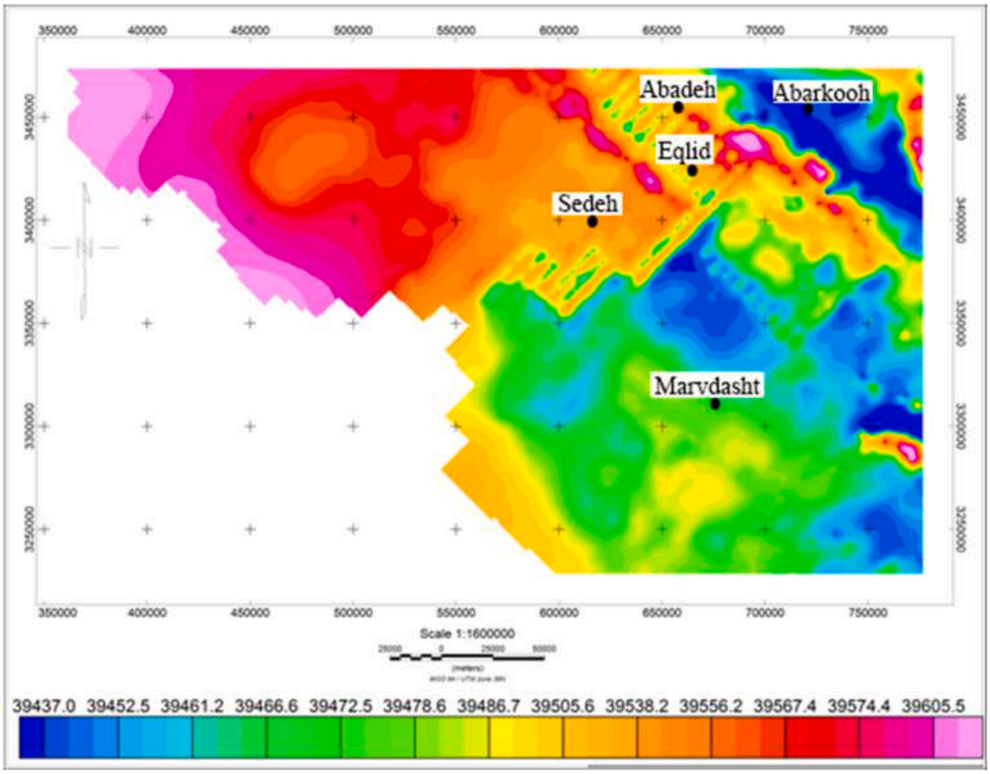


**Fig. 6.** Aeromagnetic map of the study area shows magnetic anomalies. Different colors in this map show different magnetic intensities. (For interpretation of the references to color in this figure legend, the reader is referred to the Web version of this article.)

sedimentary basins than the topography (Okiwelu et al., 2012; Mohammadzadeh-Moghaddam et al., 2015; Olasunkanmi et al., 2018). Evidence of faulting must be investigated along-strike of the detected lineaments.

### 5.3. Cross sections

Two cross-sections (Fig. 8) were constrained based on *(i)* field studies, *(ii)* Landsat images, *(iii)* geological maps provided from the National Iranian Oil Company (1:1,000,000 scale maps), and *(iv)* available cross-sections produced by the Geological Survey of Iran and the National Iranian Oil Operating Company (Repository). The length of cross-sections AA´ and BB´ are~ 130 and 38 km, respectively.

The study area is covered in the four maps with a scale of 1:100000. Names of these maps are Droudzan (provided by the Iranian Oil Operating Company), Sedeh (supplied by the National Iranian Oil Company), Sivand and Eghlid (produced by the Geological Survey of Iran). These were named as per the prominent locality these maps covered.

Cross-section AA′ runs across the Kuh-e Nabati, Kuh-e Darghook, Kuh-e Bakan, Kuh-e KushkZar, and the Kuh-e Gar anticlines. Cross section BB′ goes across the NW part of the Kuh-e Kushk Zar anticline. Cross-section AA′ indicates the effect of the faults (F3, F4, F5 and F6) extracted from the tilt filtering map. Cross-section BB′ exhibits the effect of the F4 fault alone. The cross-sections demonstrate the role of the extracted basement faults in the sequence stratigraphy (Fig. 8).

Using the 2D Move software, the kink dip domain method was applied for the preparation of the cross-sections. In this method, the dip of layers in the folds changes at a small distance. The cross-sections demonstrate that folded layers got slipped by listric faults. Therefore, fault-related drag folds (Mukherjee, 2014) cannot be ascertained.

The detected faults in this work were shown in the existing cross-sections. But in the previous studies the cross-sections are in shallow depth and the detected faults were not considered as the basement faults. In other words, the attitude of the detected faults at a higher depth was not clear in the previous cross-sections. In this research, we indicate the faults have cut the basement at 9000–12000 m depths.

## 6. Results

### 6.1. Magnetic lineaments

Local anomalies of the magnetic data in the tilt filtering map indicate the location of the magnetic lineaments (Fig. 9). Magnetic lineaments can be considered as faults if there are evidence for faulting on the tilt filtering map or at the surface. In this work, lineaments were extracted on the tilt filtering map. Then the evidence of their surficial effects was studied.

Most of the extracted lineaments correspond to the given faults. The faults caused complexity in the structures in this area. In the HD-TDR map, these detected faults are visible as lineaments (e.g. F1, F2, F5 and F6) or between the different anomalies (F3 and F4). Detected faults in the HD-TDR map show the NE-SW and NW-SE trends in the study area (Fig. 9A). Rose diagram of the detected faults indicates NW-SE as their dominant trend (Fig. 9B).

### 6.2. Detected faults and their surficial effects

#### 6.2.1. General points

The folds visible on the DEM (Fig. 10) trend NW in the NW part of the Fars province. However, some anticlines indicate a deflection of axial trace along the NE–SW faults. Detected faults on the tilt filtering map were overlaid on the DEM (Fig. 10) and the cross-sections (Fig. 8). This correlation shows the surficial effects of the main detected faults at the surface(as deflection of folds), although the faults are blind.

The surficial effects of few major detected faults are labeled (F1– F6; Figs. 9 and 10). F1 and F2 trend NE and F3–F6 trend NW. The major NW-trending anticlines are also visible on the DEM (Fig. 10) and in the cross-sections. These folds are Kuh-e Nabati, Kuh-e Darghook, Kuh-e Bakan,

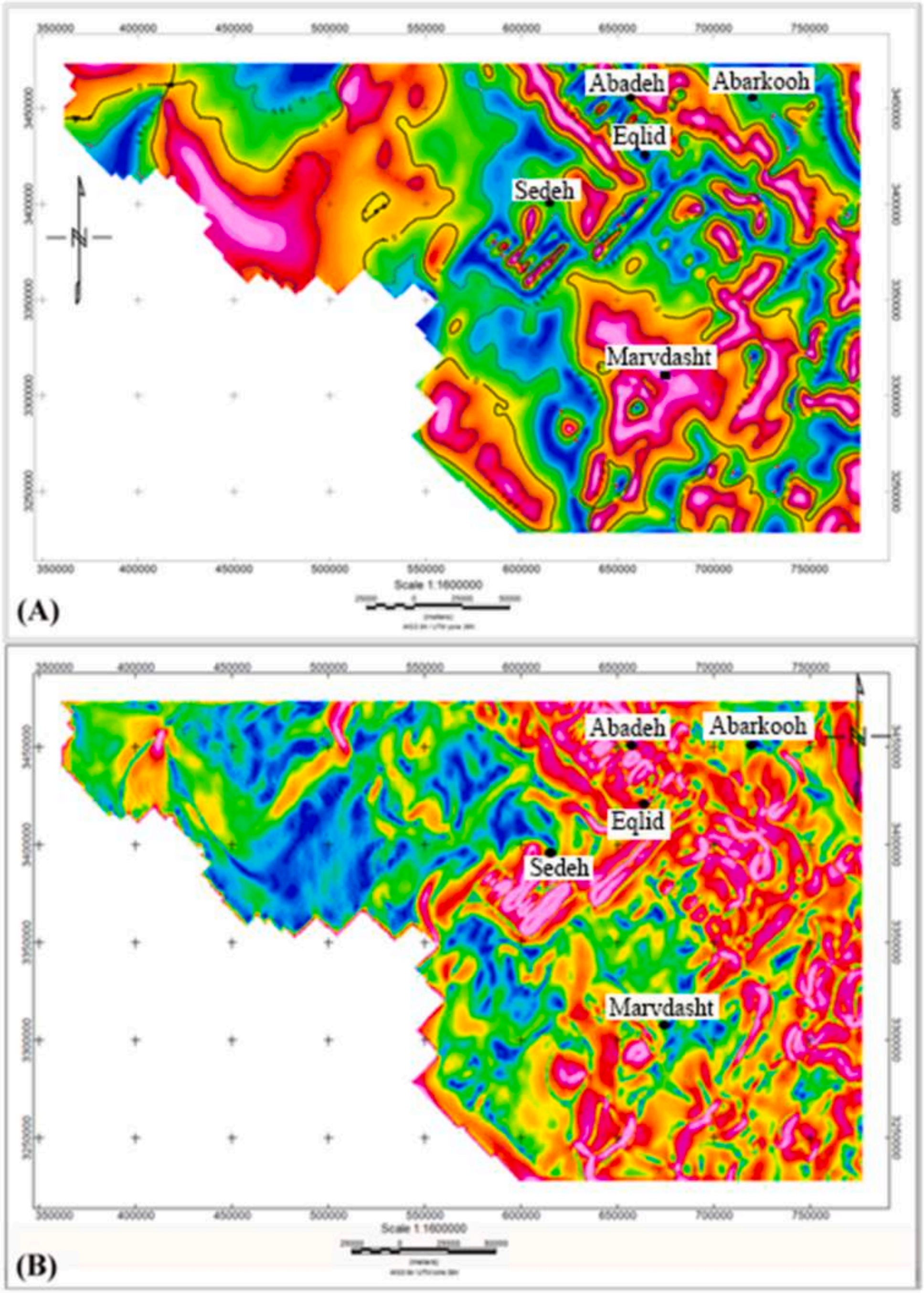


**Fig. 7.** TDR (A) and HD - TDR (B) maps of the study area. TDR and HD-TDR maps indicate the border of magnetic mass and lineaments, respectively.

Kuh-e KushkZar and Kuh-e Gar anticlines (Figs. 5 and 10). Few of these folds were presented in the geologic maps of the previous workers (Repository). Based on detail geological map (provided by Iranian Oil Operating Company, Droudzan sheet with a scale 1:100000), the basement fault in the SW part of the Kuh-e Kalb Ali anticline is a reverse fault.

The anticlines Kuh-e Tang-e Siah, Kuh-e Darghook, Kuh-e Nabati, Kuh-e Tange Goorak and Kuh-e Basiram anticlines trend NW-SE. These anticlines developed during the shortening of the Zagros orogeny. The forelimbs of these anticlines are cut by reverse faults. The interlimb angles of the Kuh-e Tang-e Siah and Kuh-e Darghook anticlines are more than those of the anticlines Kuh-e Nabati, Kuh-e Tange Goorak and the Kuh-e Basiram. In general, the anticlines are tighter in the NE part of the cross-section towards the High Zagros Zone. This is because deformation intensifies towards the High Zagros zone and the folds are tighter and more numerous (Bahroudi and Koyi, 2003; Sherkati et al., 2006). The forelimbs of the Kuh-e Tang-e Siah, Kuh-e Darghook and Kuh-e Nabati are cut by the F4, F5 and F6 reverse faults, respectively. The Kuh-e Tange Goorak and the Kuh-e Basiram anticlines are located outside the study area.

#### 6.2.2. *Surficial effects of the NE-trending subsurface faults*

We document a clockwise rotation in the Sarvak Formation and an offset of ~2.5 km of the anticlinal axes across the detected NE-trending basement faults (Fig. 10). These faults manifest as magnetic lineaments. The main detected NE-trending basement faults are $F_1$ and $F_2$. The displacement of the $F_1$ with respect to $F_2$ is probably due to the NW-trending $F_4$. The offsets of the Kuh-e Tang Siah anticline and the

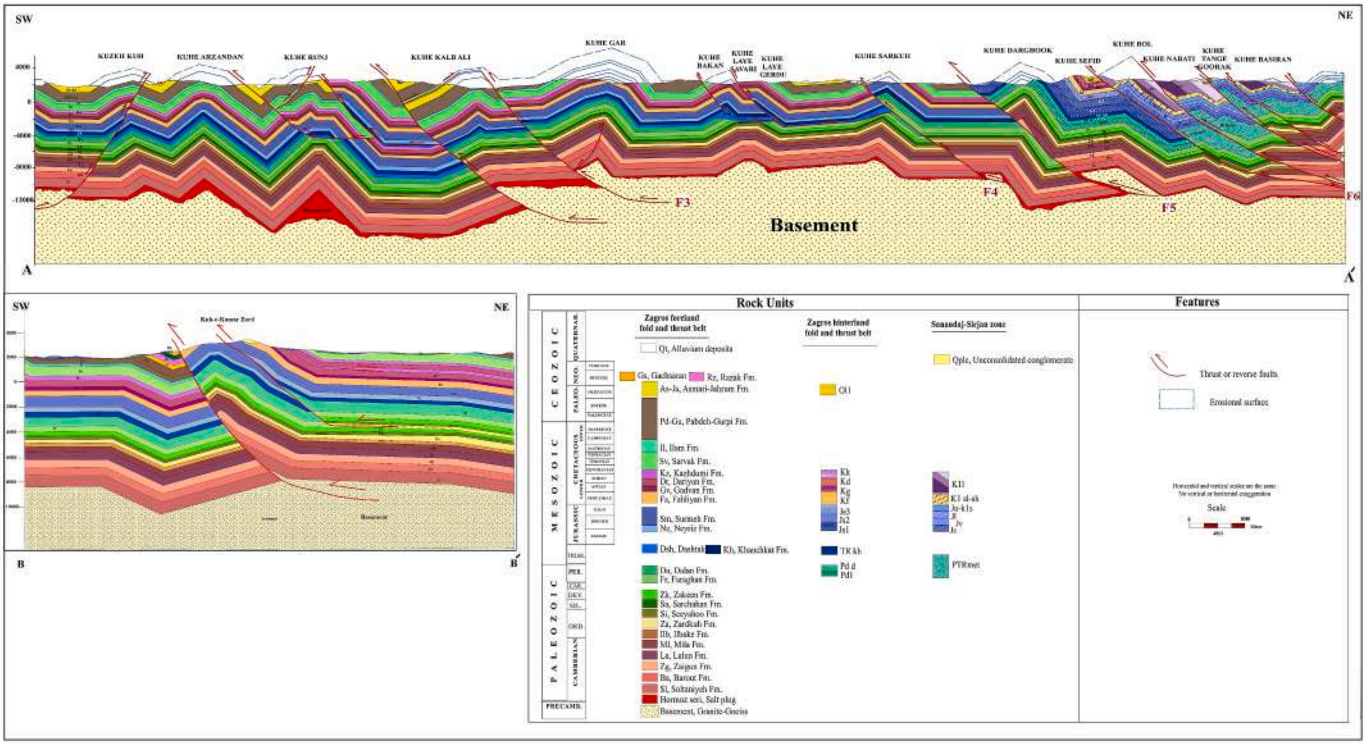


**Fig. 8.** Two NE-trending cross-sections along AA′ and BB′. Location of sections and legend of formations shown in Fig. 5B.The length of cross-sections AA´ and BB´ are~ 130 and 38 km, respectively. Cross-sections AA´ and BB´ are drawn in elevation 2000 m at the surface to a depth of 10000 m (cross-section BB´) and 14000 m (cross-section AA´).

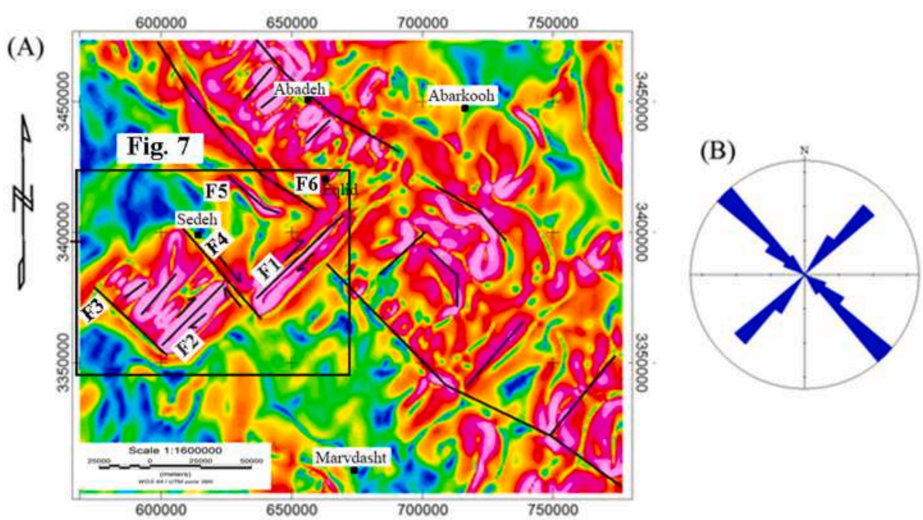


**Fig. 9.** (A) Extracted magnetic lineaments using the tilt filtering of magnetic data in the NW of Fars province and, (B) Rose diagram of the detected faults indicates two main trends: NW-SE (dominant) and NE-SW trending. Box on the tilt filtering map shows the location of Fig. 10.

deflection of the Kuh-e Gand Booie and Kuh-e Darghook anticlines occur as $F_1$ on the DEM. Deflection of the southwestern termination of the Kuh-e Bakan along the $F_2$ suggests its left-lateral slip.

### *6.2.3. Surficial effects of the NW-trending subsurface faults*

In the study area, the foreland-dipping limb of the anticlines (e.g., Kuh-e Gar, Kuh-e KushkZar, Kuh-e Darghook and Kuh-e Nabati anticlines) is cut by NW-trending F3–F6 (Fig. 10). F6 is the Zagros Main Thrust that separates the Far province from the Sanandaj-Sirjan metamorphic zone. In the Zagros belt, the NW-trending faults have cut the frontal limb of the anticlines and parallel the axial planes. These faults are listric within the basement with their dips decreasing with depth (Sarkarinejad and Goftari, 2019).

Enhancement of the NW-trending structures in the tilt filtering map plausible indicates that these deep-seated NW-SE faults originated from the basement and propagated towards the surface during the genesis of the anticlines. In other words, progressive compression leading to anticlines propagated these faults towards the surface and has cut the forelimb of the anticlines in the sedimentary cover.

The NW-SE faults could be detected in the sequence stratigraphy (Fig. 8). Slip is observed in the Late Cretaceous Ilam Formation in the upper part of the cross-section (near the surface) to the Precambrian

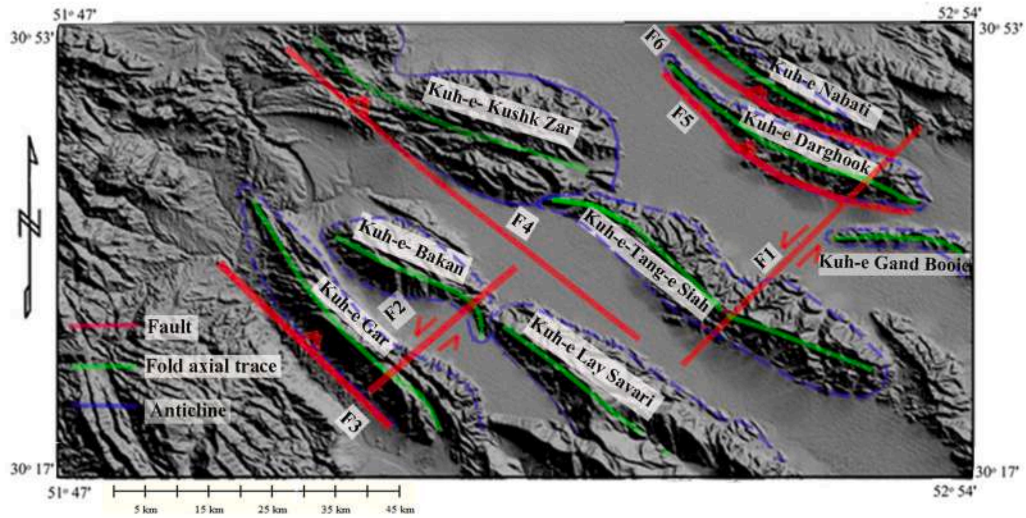


**Fig. 10.** Comparison of the detected basement faults with the anticline morphology at the surface on the Digital Elevation Model (DEM). Anticlines are deflected.

basement and across F1–F6. Slip in the basement is ~1000–4000 m across the detected NW-SE detected faults. F5 and F6 have cut the forelimbs of the Kuh-e Darghook and Kuh-e Nabati anticlines, respectively, at a high-angle. F3 and F4 have cut at a high-angle the forelimb of the Kuh-e Kushk Zar and Kuh-e Gar anticlines, respectively. F3is associated with the significant slip of the layers that and also continue within the basement.

Variations in the thicknesses of the layers are due to F4, F5 and F6 (Fig. 8). The Triassic Dashtak Formation with evaporate facies in the footwall of F4 is omitted in the hangingwall block of this fault. In the hangingwall of F4, Khaneh-Kat Formation with carbonate facies thickened within this time. Also, facies and thickness (1000–4000 m along NE-SW) in the sequence stratigraphy have shown changes in Permian, Jurassic and Lower Cretaceous deposits along with F5 and F6 (Fig. 8).

## 7. Discussions

Detection of deep-seated basement faults as the controlling factor of the structural style of the fold–and-thrust belts is a necessary step to predict their long and short-term dynamics, including seismic hazard, and to assess their potential of hydrocarbon exploration (e.g., Reeves, 1990; Misra and Mukherjee, 2015; Lacombe and Bellahsen, 2016). The studies on the basement faults in the fold-and-thrust belts, such as the Zagros Fold-Thrust Belt, have often been performed using indirect information, such as gravity (Aydogan 2011), magnetic data (e.g., Ndougsa-Mbarga et al., 2012), topographic anomalies (Leturmy et al., 2010), drainage network patterns (Leturmy et al., 2010), seismic tectonics studies (e.g,Jackson, 1980; Roustaei et al., 2010) etc.

Several techniques exist to interpret the aeromagnetic data and to detect the lineaments (Saibi et al., 2016; Boutirame et al., 2019). These techniques are consistent with Reduction To Pole (RTP) filtering and Tilt filtering.

In the Zagros belt, especially in the Fars province, the basement has controlled the surface structures only at the latest age of the tectonic evolution of the belt (e.g., Sherkati and LetouzeyJ, 2004; Leturmy et al., 2010). In other words, the current thick-skinned style of the Zagros deformation succeeded a more general thin-skinned orogenic phase (Oveisi et al., 2009). This chronology is well illustrated by the spectacular structural interference where the folds are cut by the late oblique basement faults. These faults are covered by the Quaternary sediments at the surface and are dominantly blind. The mentioned faults, e.g., the Zagros Mountain Front Fault and the Zagros Main Thrust Fault (Fig. 2), trend NW. Such a pattern repeats throughout the Fars province (Leturmy et al., 2010).

Several authors have attributed the deformation of the Zagros sedimentary cover to the pre-existing basement faults (review in Table 3). Basement faults in the Zagros belt are usually beneath the sedimentary units within ~ 7–14 km depth and rarely reach the surface (Berberian, 1995). In the Fars province, the folded sediment cover was detached in the Hormuz salt over the Precambrian basement. The basement was also shortened but how far it governed the tectonics has remained indeterminate (Mouthereau et al., 2012).

The anticlines trend NW in the study area. Some of the anticlines (e.g., Kuh-e Tang-e Siah, Kuh-e Bakan, and Kuh-e Gand Booie anticlines) deflect their axial trends along the NE-SW trending faults possibly due to the drag effect of those faults (Mukherjee, 2014). Such deflections are frequently observed in the fold axes in the Fars province and have been classically interpreted as a result of strike-slip along the underlying basement faults that manifests so in the cover (RicouL, 1974; Hessami et al., 2001). The influence of these strike-slip faults in accommodating the cover deformation has also been demonstrated in several parts of the Zagros fold-and-thrust belt (e.g. Kuhn and Reuther, 1999; Sarkarinejad et al., 2018a, 2018b; Razavi Pash et al., 2020). Lateral offset of the fold axes and geomorphic features along the strike-slip faults in the Zagros Fold-Thrust Belt has also been frequently demonstrated (e.g. Barzegarf, 1994; Hessami et al., 2001; Koyi et al., 2016).

The NE-trending faults deflect and offset the anticlinal axes as the left-lateral slip. On the other hand, the NW-trending faults cut the forelimb of the anticlines and slipped layers right-laterally as thrust. These faults usually act as blind ramps (Leturmy et al., 2010).

Overall in the Zagros belt, and also in the Fars province, the NW-SE trending faults are the thrusts/reverse faults, or thrusts with the dextral strike-slip component, such as the Main Zagros Thrust (Hessami et al., 2001). They cut the forelimb of the folds as the thrust faults in the Zagros. In the study area, these faults have cut the forelimb of the Kuh-e Nabati, Kuh-e Darghook, Kuh-e Tang-e Siah, Kuh-e Bakan, Kuh-e KushkZar, and the Kuh-e Gar anticlines. The Kuh-e Bakan, and Kuh-e Laye anticlines developed above the middle detachment (Dashtak Evaporation Formation) are typical breakthrough fault-propagation folds.

## 8. Conclusions

Deep-seated basement faults mainly govern structural style in the NW part of the Fars province. In this region, NW- SE and NE- SW are the trends of the basement faults. The NW-SE trending faults are sub-parallel to the Zagros Fold-Thrust Belt. Anticlinal axes deflected at the surface due to the faulting of the basement. The deep-seated faults changed the

**Table 3**
A list of references related to the effect of pre-existing basement faults on the deformation of the Zagros sedimentary cover.

| Reference | Studied terrain | Applied Method | Findings |
|---|---|---|---|
| Hessami et al. (2001) | Zagros Fold and Thrust Belt | Landsat satellite images, in conjunction with the spatial distribution of earthquakes and their focal mechanism solutions | Reactivated basement faults, which are inherited from the Pan-African construction phase, controlled both deposition of the Phanerozoic cover before Tertiary-Recent deformation of the Zagros and probably the entrapment of hydrocarbons on the NE margin of Arabia and in the Zagros area |
| Sherkati and LetouzeyJ (2004) | Dezful Embayment in the central Zagros belt | Interpretation of the seismic profiles, Isopach maps of Formations and stratigraphic correlation | Geometric and kinematic evolution of the Zagros fold thrust belt was strongly affected by reactivation of pre-existing basement faults |
| Mouthereau et al. (2006) | The Zagros folded belt (Fars, Iran) | Constraints from topography and critical wedge modelling | Basement thrusting produce locally significant deformation in the cover |
| Abdollahie Fard et al. (2006) | Abadan Plain and the Dezful Embayment in the central Zagros belt | Interpretation of the seismic profiles | Deep seated anticlines in the Zagros belt (in the Abadan Plain and the Dezful Embayment) show the basement is involved in the faulting. |
| Leturmy et al. (2010) | Fars Arc of the Zagros (Iran) | Morphotectonics study | Basement involvement occurred at a late stage of deformation (early detachment folds are cut by late oblique basement faults) |
| Nissen et al. (2011) | Zagros fold-and-thrust belt | Interpretation of earthquake data: focal mechanisms, magnitudes and depth | Local network earthquake data demonstrate that microseismicity occurs within the basement (activity of basement faults). |
| Razavi Pash et al. (2021) | BalaRud Fault in Central Zagros | Analogue Modelling | The BalaRud Fault as oblique basement has been controlled the deformation style on the border of the northern Dezful Embayment and Southern Lurestan province |

thickness of their adjacent litho-units. These faults are the main controlling factor of tectonics in the NW part of the Fars province. In other words, thick-skinned tectonics dominated the area.

## Declaration of competing interest

The authors declare the following financial interests/personal relationships which may be considered as potential competing interests: Soumyajit Mukherjee reports financial support was provided by Indian Institute of Technology Bombay. Soumyajit Mukherjee reports a relationship with Indian Institute of Technology Bombay that includes: employment. Soumyajit Mukherjee has patent None pending to None. None.

## Acknowledgements

We are indebted to the Geological Survey of Iran for providing magnetic data. CPDA grant (IIT Bombay) supported SM. We thank Luigi Tosi, Associate Editor, and the reviewers Victor Alania and Anonymous for comments.

## Appendix A. Supplementary data

Supplementary data to this article can be found online at https://doi.org/10.1016/j.marpetgeo.2021.105292.

## References

Abdollahie Fard, I., Braathen, A., Mokhtari, M., Alavi, S.A., 2006. Interaction of the Zagros fold–thrust belt and the arabian-type, deep-seated folds in the abadan plain and the dezful embayment, SW Iran. Petrol. Geosci. 12 (4), 347–362.
Agard, P., Omrani, J., Jolivet, L., Whitechurch, H., Vrielynck, B., Spakman, W., Monié, P., Meyer, B., Wortel, R., 2011. Zagros orogeny: a subduction-dominated process. Geol. Mag. 148 (5–6), 692–725.
Ali, M.Y., Fairhead, J.D., Green, C.M., Noufal, A., 2017. Basement structure of the United Arab Emirates derived from an analysis of regional gravity and aeromagnetic database. Tectonophysics 712, 503–522.
Arisoy, M.O., Dikmen, U., 2013. Edge detection of magnetic sources using enhanced total horizontal derivative of the tilt angle. Bull. Earth Sci. Appl. Res. Cent. Hacet. Univ. 34, 73–82.
Ariyo, S., Coker, J.O., Alaka, A.O., Adenuga, O.A., Bayewu, O.O., 2020. Integration of magnetic residuals, derivates and located euler deconvolution for structural and geologic mapping of parts of the precambrian gneisses of Ago-Iwoye, Southwestern Nigeria. GeoScience Engineering 66 (1), 1–32.
Authemayou, C., Chardon, D., Bellier, O., Malekzadeh, Z., Shabanian, E., Abbassi, M.R., 2006. Late Cenozoic partitioning of oblique plate convergence in the Zagros fold-and-thrust belt (Iran). Tectonics 25, TC3002.
Authemayou, C., Bellier, O., Chardon, D., Benedetti, L., Malekzade, Z., Claude, C., Angeletti, B., Shabanian, E., Abbassi, M.R., 2009. Quaternary slip-rates of the Kazerun and the Main Recent Faults: active strike-slip partitioning in the Zagros fold-and-thrust belt. Geophys. J. Int. 178 (1), 524–540.
Aydogan, D., 2011. Extraction of lineaments from gravity anomaly maps using the gradient calculation: application to Central Anatolia. Earth Planets Space 63 (8), 903–913.
Bahroudi, A., Koyi, H., 2003. Effect of spatial distribution of Hormuz salt on deformation style in the Zagros fold and thrust belt: an analogue modelling approach. J. Geol. Soc. 160 (5), 719–733.
Bahroudi, A., Talbot, C.J., 2003. The configuration of the basement beneath the Zagros basin. J. Petrol. Geol. 26 (3), 257–282.
Barzegarf, 1994. Basement fault mapping of e Zagros folded belt (SW Iran) based on space-born remotely sensed data. Proceedings of the 10th Thematic Conference on Geologic Remote Sensing: Exploration, Environment and Engineering, pp. 455–466 (San Antonio, Texas).
Berberian, M., 1995. Master blind thrust faults hidden under the Zagros folds: active basement tectonics and surface morphotectonics. Tectonophysics 241, 193–224.
Blakely, R.J., 1995. Potential Theory in Gravity and Magnetic Applications. Cambridge Univ. Press, New York.
Boutirame, I., Boukdir, A., Akhssas, A., Manar, A., 2019. Geological structures mapping using aeromagnetic prospecting and remote sensing data in the karstic massif of benimellal atlas, Morocco. Bulletin of the Mineral Research and Exploration 160 (160), 1–10.
Cordell, L., Grauch, V.J.S., 1985. Mapping basement magnetization zones from aeromagnetic data in the San Juan Basin, New Mexico. The Utility of Regional Gravity and Magnetic Anomaly Maps. Society of Exploration Geophysicists, pp. 181–197.
Crawford, B.L., Betts, P.G., Aillères, L., 2010. An aeromagnetic approach to revealing buried basement structures and their role in the Proterozoic evolution of the Wernecke Inlier, Yukon Territory, Canada. Tectonophysics 490 (1–2), 28–46.
DeMets, C., Gordon, R.G., Argus, F., SteinS, 1990. Current plate motions. Geophysics Journal International101 425, 478.
Geng, M., Ali, M.Y., Fairhead, J.D., Bouzidi, Y., Barkat, B., 2020. Morphology of the basement and Hormuz salt distribution in offshore Abu Dhabi from constrained 3-D inversion of gravity and magnetic data, Tectonophysics791, 228563.
Hessami, K., Koyi, H.A., Talbot, C.J., 2001. The significance of strike-slip faulting in the basement of the Zagros fold and thrust belt. J. Petrol. Geol. 24, 5–28.
HuberH, 1977. Geological Map of Iran, 1: 1,000,000 with Explanatory Note. National Iranian Oil Company. Exploration and Production Affairs, Tehran.

Ibraheem, I.M., Haggag, M., Tezkan, B., 2019. Edge detectors as structural imaging tools using aeromagnetic data: a case study of sohag area, Egypt. Geosciences 9 (5), 211.
Ikioda, P.E., Ofoegbu, C.O., Uko, E.D., Ayanninuola, O.S., 2021. Estimation of TheStructural pattern and sedimentary thickness over Part Of anambra basin, Nigeria UsingAeromagnetic data. Pak. J. Geriatr. 5, 8–12.
Jackson, J.A., 1980. Reactivation of basement faults and crustal shortening in orogenic belts. Nature 283, 343–346.
Jacobi, R.D., 2002. Basement faults and seismicity in the appalachian basin of New York state. Tectonophysics 353 (1–4), 75–113.
Jahani, S., Callot, J.P., LetouzeyJ, F rizon de Lamotte, D., 2009. The eastern termination of the Zagros Fold-and-Thrust Belt, Iran: structures, evolution, and relationships between salt plugs, folding, and faulting. Tectonics 28 (6).
JahaniS, 2009. Salt tectonics, folding and faulting in the Eastern Fars and southern offshore provinces (Iran). Université de Cergy – Pontoise. Ph.Dthesis.
Koyi, H., Nilfouroushan, F., Hessamik, 2016. Modeling role of basement block rotation and strike-slip faulting on structural pattern in cover units of fold-and-thrust belts. Geol. Mag. 153 (5/6), 827–844.
Kuhn, D., Reuther, C.D., 1999. Strike-slip faulting and nested block rotations: structural evidence from the Cordillera de Domeyko, northern Chile. Tectonophysics 313, 383–398.
Lacombe, O., Bellahsen, N., 2016. Thick-skinned tectonics and basement-involved fold–thrust belts: insights from selected Cenozoic orogens. Geol. Mag. 153 (5–6), 763–810.
Lacombe, O., Mouthereau, F., 2002. Basement-involved shortening and deep detachment tectonics in forelands of orogens: insights from recent collision belts (Taiwan, Western Alps, Pyrenees). Tectonics 21 (4), 1–12.
Lacombe, O., Mouthereau, F., Kargar, S., Meyer, B., 2006. Late Cenozoic and modern stress fields in the western Fars (Iran): implications for the tectonic and kinematic evolution of central Zagros. Tectonics 25 (1).
Lacombe, O., Grasemann, B., Simpson, G., 2011. Introduction: geodynamic evolution of the Zagros. Geodynamic magazine 148 (5–6), 689–691.
Lenhart, A., Jackson, C.A.L., Bell, R.E., Duffy, O.B., Gawthorpe, R.L., Fossen, H., 2019. Structural architecture and composition of crystalline basement offshore west Norway. Lithosphere 11 (2), 273–293.
Letouzey, J., Sherkati, S., 2004. Salt movement, tectonic events, and structural style in the central Zagros fold and thrust belt (Iran). Salt-sediment Interactions and Hydrocarbon Prospectivity: 24th Annual Research Conference, Gulf Coast Section. SEPM Foundation, pp. 444–463.
Leturmy, P., Molinaro, M., de Lamotte, D.F., 2010. Structure, timing and morphological signature of hidden reverse basement faults in the Fars Arc of the Zagros (Iran). Geological Society, London, Special Publications 330 (1), 121–138.
Lin, B., Zhang, X., Xu, X., Yuan, J., Neng, Y., Zhu, J., 2015. Features and effects of basement faults on deposition in the Tarim Basin. Earth Sci. Rev. 145, 43–55.
Lyatsky, H., Pana, D., Olson, R., Godwin, L., 2004. Detection of subtle basement faults with gravity and magnetic data in the Alberta Basin, Canada: a data-use tutorial. Lead. Edge 23 (12), 1282–1288.
Masson, F.D.R., Anvari, M., Djamour, Y., Walpersdorf, A., Tavakoli, F., Daignières, M., Nankali, H., Van Gorp, S.B., 2007. Large-scale velocity field and strain tensor in Iran inferred from GPS measurements: new insight for the present-day deformation pattern within NE Iran. Geophys. J. Int. 170, 436–440.
McClusky, S.M., Reillinger, R., Mahmoud, S., BenSari, D., Tealeb, A., 2003. GPS constraints on Africa (Nubia) and Arabia plate motions. Geophysics Journal International 155, 126–138.
Miller, H.G., Singh, V., 1994. Potential field tilt, A new concept for location of potential field sources. J. Appl. Geophys. 32, 213–217.
Misra, A.A., Mukherjee, S., 2015. Tectonic inheritance in continental rifts and passive margins. Springerbriefs in Earth Sciences. ISBN 978-3-319-20576-2.
Mohammadzadeh Moghaddam, M.M., Sabseparvar, M., Mirzaei, S., Heydarian, N., 2015. Interpretation of aeromagnetic data to locate buried faults in North of Zanjan Province. Iran. J. Geophys. Rem. Sens. 4 (143).
Mouthereau, F., Lacombe, O., Meyer, B., 2006. The Zagros folded belt (Fars, Iran): constraints from topography and critical wedge modelling. Geophys. J. Int. 165 (1), 336–356.
Mouthereau, F., Tensi, J., Bellahsen, N., Lacombe, O., De Boisgrollier, T., Kargar, S., 2007. Tertiary sequence of deformation in a thin-skinned/thick-skinned collision belt: the Zagros Folded Belt (Fars, Iran). Tectonics 26 (5).
Mouthereau, F., Lacombe, O., Vergés, J., 2012. Building the Zagros collisional orogen: timing, strain distribution and the dynamics of Arabia/Eurasia plate convergence. Tectonophysics 532, 27–60.
Mukherjee, S., 2014. Review of flanking structures in meso- and micro-scales. Geol. Mag. 151, 957–974.
Mukherjee, S., Talbot, C.J., Koyi, H.A., 2010. Viscosity estimates of salt in the Hormuz and Namakdan salt diapirs, Persian Gulf. Geol. Mag. 147, 497–507.
Najafi, M., Yassaghi, A., Bahroudi, A., Vergés, J., Sherkati, S., 2014. Impact of the late triassic Dashtak intermediate detachment horizon on anticline geometry in the central frontal fars, SE Zagros Fold belt, Iran. Mar. Petrol. Geol. 54, 23–36.
Ndougsa-Mbarga, T., Feumoe, A.N.S., Manguelle-Dicoum, E., Fairhead, J.D., 2012. Aeromagnetic data interpretation to locate buried faults in south-east Cameroon. Geophysica 48 (1–2), 49–63.
Ni, J., Barazangi, M., 1986. Seismotectonics of the Zagros continental collision zone and a comparison with the Himalayas. J. Geophys. Res.: Solid Earth 91 (B8), 8205–8218.
Nissen, E., Tatar, M., Jackson, J.A., Allen, M.B., 2011. New views on earthquake faulting in the Zagros fold-and-thrust belt of Iran. Geophys. J. Int. 186 (3), 928–944.
Okiwelu, A.A., Obianwu, V.I., Eze, O., Ude, I.A., 2012. Magnetic anomaly patterns, fault block tectonism and hydrocarbon related structural features in the Niger Delta basin. Journal of Applied Geology and Geophysics 2 (1), 31–46.
Olasunkanmi, N.K., Sunmonu, L.A., Adabanija, M.A., Oladejo, O.P., 2018. July. Interpretation of high-resolution aeromagnetic data for mineral prospect in Igbeti-Moro area, Southwestern Nigeria. IOP Conf. Ser. Earth Environ. Sci. 173, 012033.
Oveisi, B., lave, J., Van Der Beek, P., Carcaillet, J., Benedetti, L., Aubourg, C., 2009. Thick- and thin-skinned deformation rates in the central Zagros simple folded zone (Iran) indicated by displacement of geomorphic surfaces. Geophys. J. Int. 176, 627–654.
Razavi-Pash, R., Sarkarinejad, K., Ghoochaninejad, H.Z., Motamedi, H., Yazdani, M., 2020. Accommodation of the different structural styles in the foreland fold-and-thrust belts: northern Dezful Embayment in the Zagros belt, Iran. Int. J. Earth Sci. 1–12.
Razavi-Pash, R., Sarkarinejad, K., Sherkati, S., Motamedi, H., 2021. Analogue model of the BalaRud Fault, Zagros: an oblique basement ramp in a fold-and-thrust belt. Int. J. Earth Sci. 110 (2), 741–755.
Reeves, A., 1990. Olympic dam copper-uranium gold-silver deposit. Geol-Ogy of the Mineral Deposits of Australia and Papua New Guinea. the Australasian Institute of Mining and Metal-Lurgy, Hughes, pp. 1009–1035.
RicouL, E., 1971. Le mé tamorphisme au contact des pé ridotites de Neyriz (Zagros interne Iran): development de skarns à pyroxé ne. Bull Society Geology France 13, 146–155.
RicouL, E., 1974. L'etudege ólogique de la région de Neyriz (Zagros iranien) etl'é volutionstructurale des Zagrides. PhD thesis, Université Paris-Sud (Orsay).
Roustaei, M., Nissen, E., Abbassi, M., Gholamzadeh, A., Ghorashi, M., Tatar, M., Yamini-Fard, F., Bergman, E., Jackson, J., Parsons, B., 2010. The 2006 march 25 fin earthquakes (Iran) insights into the vertical extents of faulting in the Zagros simply folded belt. Geophys. J. Int. 181, 1275–1291.
Saibi, H., Azizi, M., Mogren, S., 2016. Structural investigations of Afghanistan deduced from remote sensing and potential field data. Acta Geophys. 64 (4), 978–1003.
Saleh, R., 2006. Reprocessing of Aeromagnetic Map of Iran. MSc thesis, Institute for Advanced Studies in Basic Sciences.
Salem, A., Williams, S., Fairhead, J.D., Ravat, D., Smith, R., 2007. Tilt-depth method: a simple depth estimation method using first-order magnetic derivatives. Lead. Edge 26 (12), 1502–1505.
Salem, A., WilliamsS, Fairhead, J.D., Ravat, D., Smith, R., 2008. Interpretation of magnetic data using tilt-angle derivatives. J. Appl. Geophys. 73, L1–L10.
Sarkarinejad, K., Goftari, F., 2019. Thick-skinned and thin-skinned tectonics of the Zagros orogen, Iran: constraints from structural, microstructural and kinematics analyses. J. Asian Earth Sci. 170, 249–273.
Sarkarinejad, K., Razavi Pash, R., Motamedi, H., Yazdani, M., 2018a. Deformation and kinematic evolution of the subsurface structures: Zagros foreland fold-and-thrust belt, northern Dezful Embayment, Iran. Int. J. Earth Sci. 107, 1287–1304.
Sarkarinejad, K., Zafarmand, B., Oveisi, B., 2018b. Evolution of the stress fields in the ZagrosForeland Folded Belt using focal mechanisms and kinematic analyses: the case of the Farssalient, Iran. Int. J. Earth Sci. 107 (2), 611–633.
Sepehr, M., Cosgrove, J.W., 2005. Role of the KazerunFault Zone in the Formation and Deformation of the Zagros Fold-Thrust Belt, Iran. Tectonics24, p. TC5005.
Shah, A.K., Crain, K., 2018. Aeromagnetic data reveal potential seismogenic basement faults in the induced seismicity setting of Oklahoma. Geophys. Res. Lett. 45 (12), 5948–5958.
Sherkati, S., LetouzeyJ, 2004. Variation of structural style and basin evolution in the central Zagros (Izeh zone and Dezful Embayment), Iran. Journal of Marine and Petroleum Geology 21, 535–554.
Sherkati, S., Letouzey, J., Frizon de Lamotte, D., 2006. The Central Zagros fold-thrust belt (Iran) : new insights from seismic data, field observation and sandbox modeling. Tectonics 25, TC4007.
Talebian, M., Jackson, J., 2004. A reappraisal of earthquake focal mechanisms and active shortening in the Zagros mountains of Iran. Geophys. J. Int. 156, 506–526.
Teknik, V., Ghods, A., 2017. Depth of magnetic basement in Iran based on fractal spectral analysis of aeromagnetic data. Geophys. J. Int. 209 (3), 1878–1891.
Verduzco, B., FairheadJ, D., GreenC, M., MacKenzie, C., 2004. New insights into magnetic derivatives for structural mapping. Lead. Edge 23, 116–119.
Vernant, 2004. Present-day crustal deformation and plate kinematics in the Middle East constrained by GPS measurements in Iran and northern Oman. Geophys. J. Int157, 381–398.
Wang, Z., Zhou, H., Wang, X., Jing, X., 2015. Characteristics of the crystalline basement beneath the Ordos Basin: constraint from aeromagnetic data. Geoscience Frontiers 6 (3), 465–475.